Prepared for submission to JHEP

Two-gluon and trigluon glueballs from dynamical holography QCD

Yidian Chen[a], **Mei Huang**[a,b]
[a] **Institute of High Energy Physics, Chinese Academy of Sciences, Beijing, China**
[b] **Theoretical Physics Center for Science Facilities, Chinese Academy of Sciences, Beijing, China**

Abstract: We study the scalar, vector and tensor two-gluon and trigluon glueball spectra in the framework of 5-dimension dynamical holographic QCD model, where the metric structure is deformed self-consistently by the dilaton field. For comparison, the glueball spectra are also calculated in the hard-wall and soft-wall holographic QCD models. In order to distinguish glueballs with even and odd parities, we introduce the positive and negative coupling between the dilaton field and glueballs, and for higher spin glueballs, we introduce a deformed 5-dimension mass. With this set-up, there is only one free parameter from the quadratic dilaton profile in the dynamical holographic QCD model, which is fixed by the scalar glueball spectra. It is found that the two-gluon glueball spectra produced in the dynamical holographic QCD model are in good agreement with lattice data. Among six trigluon glueballs, the produced masses for $1^{\pm-}$ and 2^{--} are in good agreement with lattice data, and the produced masses for 0^{--}, 0^{+-} and 2^{+-} are around 1.5 GeV lighter than lattice results. This result might indicate that the three trigluon glueballs of 0^{--}, 0^{+-} and 2^{+-} are dominated by three-gluon condensate contribution.

Keywords: Glueball, holographic QCD model

Contents

1 Introduction

Quantum chromodynamics (QCD) is accepted as the fundamental theory of describing strong interaction. In the high energy regime, QCD has the property of asymptotic freedom and perturbative QCD calculations have been tested with high precision. However, in the low energy regime, the nonperturbative aspect related to QCD vacuum properties and hadron spectra remains as outstanding challenge. The nonabelian feature of QCD makes it possible to form bound states of gauge bosons, i.e. glueballs (gg, ggg, etc.) [1]. The gauge field plays a more important dynamical role in glueballs than that in the standard hadrons, therefore study particles like glueballs offers a good opportunity of understanding nonperturbative aspects of QCD.

The glueball spectrum has attracted much attention more than three decades [1], and it has been widely investigated by using various non-perturbative methods. For example, from first principles calculation by using lattice QCD [2–6], by using flux tube model [7] as well as by using QCD sum rules [8–10]. For more information, please refer to review papers [11].

The discovery of the gravity/gauge duality, or anti-de Sitter/conformal field theory (AdS/CFT) correspondence [12–14] offers a new possibility to tackle the difficulty of strongly coupled gauge theories, for reviews see Ref. [15]. In recent decades, many efforts have been invested from both top-down and bottum-up approaches in examining nonperturbative QCD properties, e.g., QCD equation of state, phase transitions, fluid properties of quark-gluon plasma [16], meson spectra [17–19], baryon spectra [20], as well as in the glueball sector [21–25]. It is expected that the holography approach can shed some light on our understanding of the nonperturbative aspects of QCD.

QCD is a non-conformal gauge theory, and the Sakai-Sugimoto (SS) model [26] is one of the most successful non-conformal top-down holographic QCD models. The glueball spectra in the Sakai-Sugimoto model has been investigated in literatures, see Ref. [27]. Glueballs have also been widely studied by using the bottom-up approach [23], where most studies are based on hard-wall [17] and soft-wall holographic QCD models [18] with the conformal AdS_5 background metric.

A successful holographic QCD model should grasp two main features of nonperturbative QCD properties, i.e. the spontaneous chiral symmetry breaking and color charge confinement. The dynamical holographic QCD model (DhQCD) which can describe both chiral symmetry breaking and confinement has been constructed in Ref. [28–30]. In this model, the gluon dynamics background is determined by the coupling between the graviton and the dilaton field $\Phi(z)$, which is responsible for the gluon condensate and confinement, and the scalar field $X(z)$ is introduced to mimic chiral dynamics. Evolution of the dilaton field and scalar field in 5D resemble the renormalization group from ultraviolet (UV) to infrared (IR). This DhQCD model describes the scalar glueball spectra and the light meson spectral quite well [28–30]. Further studies [31–33] show that this DhQCD model can also describe QCD phase transition, equation of state of QCD matter and temperature dependent transport properties, including shear viscosity, bulk viscosity, electric conductivity as well as jet quenching parameter.

For the scalar glueball spectra, it was shown in Ref.[29] that, comparing with the results in the hard-wall and soft-wall holographic QCD models [23], the scalar glueballs including the lowest state and excited states can be surprisingly well described in the DhQCD model . However, the scalar glueball 0^{++} has the same quantum number as the scalar quarkonium $\bar{q}q$ and tetraquark $\bar{q}q\bar{q}q$ [34] states, and the complexity of determining the glueball states lies in that gluonic bound states might always mix with $\bar{q}q$ and $\bar{q}q\bar{q}q$ states. For example, one has to distinguish the lightest scalar glueball state among 19 scalar mesons observed in the energy range below 2 GeV [35, 36]. Therefore, it is interesting to investigate odd glueballs with unconventional quantum numbers which cannot be carried by quark-antiquark bound states. These include $J^{PC} = 0^{--}, 0^{+-}, 2^{+-}, 3^{-+}$ glueballs, which can only be made of at-least three-gluon bound states.

This motivate us to investigate the whole glueball spectra including (scalar, vector as well as tensor glueballs and their excitations) in the framework of the DhQCD model. The paper is organized as following: In Sec.2 we give the operators of two-gluon and trigluon glueballs. We introduce the dynamical soft-wall holographic QCD model in Sec.3, and calculate the the glueball spectra in the dynamical holographic QCD model in Sec. 4, it is found that higher-spin glueballs are very heavy comparing with lattice data, and the even and odd parities cannot be distinguished. Therefore, we introduce a deformed 5-dimension mass for higher spin glueballs, and in order to distinguish glueballs with even and odd parities, we introduce the positive and negative coupling between the dilaton field and glueballs.With this set-up, we calculate the glueball spectra in the modified dynamical holographic QCD model in Sec. 5 and find that the two-gluon glueball spectra are in good agreement with lattice data and the trigluon glueball spectra agree with results from QCD sum rules. Finally, a short summary is given in Sec.6.

2 Two-gluon and trigluon glueballs

The AdS/CFT correspondence establishes a one-to-one correspondence between a certain class of $4D$ local operators in the $\mathcal{N} = 4$ superconformal gauge theory and $5D$ supergravity fields representing the holographic correspondents in the $AdS_5 \times S^5$ bulk theory. According to AdS/CFT dictionary, the conformal dimension of a (f-form) operator on the ultraviolet (UV) boundary is related to the M_5^2 of its dual field in the bulk as follows [12–14] :

$$M_5^2 = (\Delta - f)(\Delta + f - 4) \, . \tag{2.1}$$

In the bottom-up approach, for example in the holographic QCD models, one can expect a more general correspondence, i.e. each operator $\mathcal{O}(x)$ in the 4D field theory corresponds to a field $O(x, z)$ in the 5D bulk theory. To investigate the glueball spectra, we consider the lowest dimension operators with the corresponding quantum numbers and defined in the field theory living on the $4D$ boundary. We show the two-gluon and trigluon glueball operators and their corresponding $5D$ masses in Table 1.

J^{PC}	$4D:\mathscr{O}(x)$	Δ	f	M_5^2
0^{++}	$Tr(G^2)$	4	0	0
0^{--}	$Tr(\tilde{G}\{D_{\mu_1}D_{\mu_2}G,G\})$	8	0	32
0^{-+}	$Tr(G\tilde{G})$	4	0	0
$1^{\pm-}$	$Tr(G\{G,G\})$	6	1	15
2^{++}	$Tr(G_{\mu\alpha}G_{\alpha\nu}-\frac{1}{4}\delta_{\mu\nu}G^2)$	4	2	4
2^{++}	$E_i^aE_j^a-B_i^aB_j^a-trace$	4	2	4
2^{-+}	$E_i^aB_j^a+B_i^aE_j^a-trace$	4	2	4
$2^{\pm-}$	$Tr(G\{G,G\})$	6	2	16

Table 1. 5D mass square of two-gluon and trigluon glueballs.The operators are taken from [22] and [9, 10].

For trigluon glueball 0^{--}, the detailed structure of the operator is given in Ref. [9]

$$j^A_{0^{--}} \sim d^{abc}[g^t_{\alpha\beta}\tilde{G}^a_{\mu\nu}][\partial_\alpha\partial_\beta G^b_{\nu\rho}][G^c_{\rho\mu}], \tag{2.2}$$
$$j^B_{0^{--}} \sim d^{abc}[g^t_{\alpha\beta}G^a_{\mu\nu}][\partial_\alpha\partial_\beta \tilde{G}^b_{\nu\rho}][G^c_{\rho\mu}], \tag{2.3}$$
$$j^C_{0^{--}} \sim d^{abc}[g^t_{\alpha\beta}G^a_{\mu\nu}][\partial_\alpha\partial_\beta G^b_{\nu\rho}][\tilde{G}^c_{\rho\mu}], \tag{2.4}$$
$$j^D_{0^{--}} \sim d^{abc}[g^t_{\alpha\beta}\tilde{G}^a_{\mu\nu}][\partial_\alpha\partial_\beta \tilde{G}^b_{\nu\rho}][\tilde{G}^c_{\rho\mu}], \tag{2.5}$$

where d^{abc} stands for the totally symmetric $SU_c(3)$ structure constant and $g^t_{\alpha\beta}=g_{\alpha\beta}-\partial_\alpha\partial_\beta/\partial^2$.

The interpolating currents of the 2^{+-} oddball 2^{+-} takes the form as [10],

$$j^{2^{+-},\,A}_{\mu\alpha}(x)=g_s^3d^{abc}[G^a_{\mu\nu}(x)][G^b_{\nu\rho}(x)][G^c_{\rho\alpha}(x)]\,, \tag{2.6}$$
$$j^{2^{+-},\,B}_{\mu\alpha}(x)=g_s^3d^{abc}[G^a_{\mu\nu}(x)][\tilde{G}^b_{\nu\rho}(x)][\tilde{G}^c_{\rho\alpha}(x)]\,, \tag{2.7}$$
$$j^{2^{+-},\,C}_{\mu\alpha}(x)=g_s^3d^{abc}[\tilde{G}^a_{\mu\nu}(x)][G^b_{\nu\rho}(x)][\tilde{G}^c_{\rho\alpha}(x)]\,, \tag{2.8}$$
$$j^{2^{+-},\,D}_{\mu\alpha}(x)=g_s^3d^{abc}[\tilde{G}^a_{\mu\nu}(x)][\tilde{G}^b_{\nu\rho}(x)][G^c_{\rho\alpha}(x)]\,. \tag{2.9}$$

3 The dynamical soft-wall holographic QCD model and gluodynamics

The dynamical soft-wall holographic QCD model is described in Ref.[29]. The pure gluon part of QCD can be modelled by the 5D graviton-dilaton coupled action:

$$S_G=\frac{1}{16\pi G_5}\int d^5x\sqrt{g_s}e^{-2\Phi}\left(R_s+4\partial_M\Phi\partial^M\Phi-V_G^s(\Phi)\right), \tag{3.1}$$

where G_5 is the 5D Newton constant, g_s, Φ and V_G^s are the 5D metric, the dilaton field and dilaton potential in the string frame, respectively. The metric is chosen to be

$$g^s_{MN}=b_s^2(z)(dz^2+\eta_{\mu\nu}dx^\mu dx^\nu),\quad b_s(z)\equiv e^{A_s(z)}. \tag{3.2}$$

Under the conformal transformation

$$g^E_{MN}=g^s_{MN}e^{-4\Phi/3},\quad V_G^E=e^{4\Phi/3}V_G^s, \tag{3.3}$$

Eq.(3.1) can be rewriten in the Einstein frame

$$S_G^E = \frac{1}{16\pi G_5}\int d^5x\sqrt{g_E}\left(R_E - \frac{4}{3}\partial_M\Phi\partial^M\Phi - V_G^E(\Phi)\right). \tag{3.4}$$

The Einstein equations are

$$E_{MN} + \frac{1}{2}g^E_{MN}\left(\frac{4}{3}\partial_L\Phi\partial^L\Phi + V_G^E(\Phi)\right) - \frac{4}{3}\partial_M\Phi\partial_N\Phi = 0, \tag{3.5}$$

$$\frac{8}{3\sqrt{g_E}}\partial_M(\sqrt{g_E}\partial^M\Phi) - \partial_\Phi V_G^E(\Phi) = 0. \tag{3.6}$$

Substituting the metric of Eq.(3.2) into the above equations, we can obtain:

$$-A_E^{''} + A_E^{'2} - \frac{4}{9}\Phi^{'2} = 0, \tag{3.7}$$

$$\Phi^{''} + 3A_E^{'}\Phi^{'} - \frac{3}{8}e^{2A_E}\partial_\Phi V_G^E(\Phi) = 0, \tag{3.8}$$

where

$$b_E(z) = b_s(z)e^{-\frac{2}{3}\Phi(z)} = e^{A_E(z)}, \quad A_E(z) = A_s(z) - \frac{2}{3}\Phi(z). \tag{3.9}$$

In the string frame, the above two equations of motion are

$$-A_s^{''} - \frac{4}{3}\Phi^{'}A_s^{'} + A_s^{'2} + \frac{2}{3}\Phi^{''} = 0, \tag{3.10}$$

$$\Phi^{''} + (3A_s^{'} - 2\Phi^{'})\Phi^{'} - \frac{3}{8}e^{2A_s-\frac{4}{3}\Phi}\partial_\Phi(e^{\frac{4}{3}\Phi}V_G^s(\Phi)) = 0. \tag{3.11}$$

We take the same dilaton field as that in the KKSS model or soft-wall holographic QCD model [18], i.e.,

$$\Phi = \mu_G^2 z^2. \tag{3.12}$$

It is simple to solve the metric A_E and the dilaton potential $V_G^E(\Phi)$ in the quadratic dilaton background

$$A_E(z) = \log(\frac{L}{z}) - \log({}_0F_1(5/4, \frac{\Phi^2}{9})), \tag{3.13}$$

$$V_G^E(\Phi) = -\frac{12\,{}_0F_1(1/4, \frac{\Phi^2}{9})^2}{L^2} + \frac{16\,{}_0F_1(5/4, \frac{\Phi^2}{9})^2\Phi^2}{3L^2}, \tag{3.14}$$

with ${}_0F_1(a;z)$ the hypergeometric function.

4 Glueball spectra in the dynamical soft-wall holographic QCD model

4.1 Scalar glueballs

The 5D action for the scalar glueball $\mathscr{G}(x,z)$ in the string frame takes the form as that in the original soft-wall model [24, 25]

$$S_{\mathscr{G}} = -\int d^5x\sqrt{g_s}\frac{1}{2}e^{-\Phi}\left[\partial_M\mathscr{G}\partial^M\mathscr{G} + M_{\mathscr{G},5}^2\mathscr{G}^2\right]. \tag{4.1}$$

It is notice that the metric structure in the dynamical soft-wall model is solved from Eq. (3.8) instead of AdS_5.

The Equation of motion for the scalar glueballs $\mathscr{G}$ is given below as

$$-e^{-(3A_s-\Phi)}\partial_z(e^{3A_s-\Phi}\partial_z\mathscr{G}_n)+e^{2A_s}M_{\mathscr{G},5}^2\mathscr{G}_n=m_{\mathscr{G},n}^2\mathscr{G}_n. \tag{4.2}$$

Via the substitution $\mathscr{G}_n\to e^{-\frac{1}{2}(3A_s-\Phi)}\mathscr{G}_n$, the equation can be brought into schrödinger-like equation

$$-\mathscr{G}_n^{''}+V_{\mathscr{G}}\mathscr{G}_n=m_{\mathscr{G},n}^2\mathscr{G}_n, \tag{4.3}$$

with the 5D effective schrödinger potential

$$V_{\mathscr{G}}=\frac{3A_s^{''}-\Phi^{''}}{2}+\frac{(3A_s^{'}-\Phi^{'})^2}{4}+e^{2A_s}M_{\mathscr{G},5}^2. \tag{4.4}$$

4.2 Vector glueballs

For vector gluebalsl $\mathscr{V}$, the 5D action is

$$S_V=-\int d^5x\sqrt{g}e^{-\Phi}(\frac{1}{4}F^{MN}F_{MN}+\frac{1}{2}M_{\mathscr{V},5}^2\mathscr{V}^2), \tag{4.5}$$

where $F_{MN}=\partial_M\mathscr{V}_N-\partial_N\mathscr{V}_M$.

The equation of motion for vector glueballs $\mathscr{V}$ is

$$-e^{-(A_s-\Phi)}\partial_z(e^{A_s-\Phi}\partial_z\mathscr{V}_n)+e^{2A_s}M_{\mathscr{V},5}^2\mathscr{V}_n=m_{\mathscr{V},n}^2\mathscr{V}_n. \tag{4.6}$$

Via the substitution $\mathscr{V}_n\to e^{-\frac{1}{2}(A_s-\Phi)}\mathscr{V}_n$, the equation can be brought into schrödinger-like equation

$$-\mathscr{V}_n^{''}+V_{\mathscr{V}}\mathscr{V}_n=m_{\mathscr{V},n}^2\mathscr{V}_n, \tag{4.7}$$

with the 5D effective schrödinger potential

$$V_{\mathscr{V}}=\frac{A_s^{''}-\Phi^{''}}{2}+\frac{(A_s^{'}-\Phi^{'})^2}{4}+e^{2A_s}M_{\mathscr{V},5}^2. \tag{4.8}$$

4.3 Tensor glueballs

For tensor glueballs, the 5D action is

$$\begin{aligned}S_T=-\frac{1}{2}\int d^5x\sqrt{g}e^{-\Phi}(\ &\nabla_L h_{MN}\nabla^L h^{MN}-2\nabla_L h^{LM}\nabla^N h_{NM}+2\nabla_M h^{MN}\nabla_N h\\ &-\nabla_M h\nabla^M h+M_{h,5}^2(h^{MN}h_{MN}-h^2)),\end{aligned} \tag{4.9}$$

where $h=g^{MN}h_{MN}$. With the constraint

$$\nabla_M h^{MN}=0,\quad h=0,\quad h_{\mu\nu}=e^{2A_s}\mathscr{H}_{\mu\nu},\quad h_{Mz}=0, \tag{4.10}$$

The equation of motion for tensor glueballs $\mathscr{H}_{\mu\nu}$ is

$$-e^{-(3A_s-\Phi)}\partial_z(e^{3A_s-\Phi}\partial_z\mathscr{H}_n)+e^{2A_s}M_{\mathscr{H},5}^2\mathscr{H}_n=m_{\mathscr{H},n}^2\mathscr{H}_n. \tag{4.11}$$

Via the substitution $\mathscr{H}_n \to e^{-\frac{1}{2}(3A_s-\Phi)}\mathscr{H}_n$, the equation can be brought into schrödinger-like equation

$$-\mathscr{H}_n'' + V_{\mathscr{H}}\mathscr{H}_n = m^2_{\mathscr{H},n}\mathscr{H}_n, \tag{4.12}$$

with the 5D effective schrödinger potential

$$V_{\mathscr{H}} = \frac{3A_s'' - \Phi''}{2} + \frac{(3A_s' - \Phi')^2}{4} + e^{2A_s}M^2_{\mathscr{H},5}. \tag{4.13}$$

4.4 Numerical results

For numerical calculations, we have to fix parameters in the model. In the dynamical holographic model, there is only one free parameter, i.e., μ_G. We fix this parameter by fitting the scalar glueballs spectra from lattice results [2–5] as shown in Table 2. The lattice data in Table 2 indicates the slope of the Regge spectra is around 4GeV^2, which is equivalent to $\mu_G \simeq 1\text{GeV}$ in the dynamical holographic QCD model.

n(0^{++})	Lat1	Lat2	Lat3	Lat4	Lat5
	$N_c = 3$	$N_c = 3$	$N_c \to \infty$	$N_c = 3$	$N_c = 3$
1	1475(30)(65)	1580(11)	1480(07)	1730(50)(80)	1710(50)(80)
2	2755(70)(120)	2750(35)	2830(22)	2670(180)(130)	
3	3370(100)(150)				
4	3990(210)(180)				

Table 2. Lattice data for 0^{++}*glueball* in unit of MeV. Lat1 data from Ref.[4], Lat2 and Lat3 data from Ref.[3], Lat4 [2] and Lat5 [5] are anisotropic results.

We will also compare our results in the dynamical holographic QCD model with those in the hard-wall and soft-wall holographic QCD models. In the hard-wall holographic QCD model, the equation of motion for glueball $\mathscr{G}$ is:

$$-e^{-cA_s}\partial_z(e^{cA_s}\partial_z\mathscr{G}_n) + e^{2A_s}M^2_{\mathscr{G},5}\mathscr{G}_n = m^2_{\mathscr{G},n}\mathscr{G}_n, \tag{4.14}$$

where $c = 1$ for vector glueballs and $c = 3$ for scalar and tensor glueballs. With UV boundary condition $\mathscr{G}_n(\epsilon) = 0$, the solution is:

$$\mathscr{G}_n(z) = z^{\frac{1+c}{2}}J_n(m_{\mathscr{G},n}, z), \tag{4.15}$$

where $n = \sqrt{1 + 2c + c^2 + 4M^2_{\mathscr{G},5}}/2$ and J is Bessel function. IR boundary condition $\partial_z\mathscr{G}_n(z_m) = 0$ gives the discrete spectrum of the glueballs. Here z_m is the hard cut-off, which is the only parameter in the hard-wall model, and can be fixed by the ground state of the scalar glueball 0^{++}. When we take the mass for the lowest scalar glueball as 1730MeV, which fixes $z_m = 452\text{MeV}$ in the hard wall model.

In the soft-wall model, with the dilaton background takes the quadratic form $\Phi = \mu_G^2 z^2$ and the metric structure is still AdS_5, the Regge spectra for glueball can be derived as [24, 25]

$$m_n^2 = \mu_G^2 \left\{ 4n + c + 1 + \sqrt{(c+1)^2 + 4M_5^2} \right\}, \ n = 0, 1, 2, \cdots \tag{4.16}$$

where $c = 3$ in case of scalar and tensor and $c = 1$ in case of vector. There is also only one parameter μ_G in the soft-wall model. The Regge slope of 0^{++} glueball gives $\mu_G = 1$GeV (SW†), and the the lowest scalar glueball mass 1730MeV gives $\mu_G = 0.5$GeV (SW††).

J^{PC}	Lattice	HW	SW†	SW‡	DSW
0^{++}	1475-1730	1730	1730	2828	1593
0^{*++}	2670-2830	3168	2119	3464	2618
0^{**++}	3370	4593	2447	4000	3311
0^{***++}	3990	6016	2735	4472	3877

Table 3. The mass spectra of 0^{++} glueballs in the dynamical soft-wall model, compared with combined lattice data [2–5], and hard-wall model ($z_m = 452$MeV), soft-wall model with SW† indicates μ_G is fixed by lowest mass of 0^{++} glueball, and SW‡ indicates μ_G is fixed by Regge slope of 0^{++} glueball. The unit is in MeV.

Table 3 shows scalar glueball spectra in the dynamical soft-wall holographic QCD model, and the results are compared with combined lattice data [2–5] as well as hard-wall and soft-wall models, respectively. It is found that the hard-wall model cannot produce Regge spectra, and the soft-wall model cannot simultaneously produce the correct Regge slope and the ground state of the scalar glueball. As it was shown in Ref. [29], the Regge slope and the ground state of the scalar glueball can be correctly produced in the dynamical soft-wall holographic QCD model with only one parameter.

With the parameter fixed by the scalar glueball, we calculate the vector and tensor glueball masses in the dynamical soft-wall model and compare with lattice data as well as results from hard-wall and soft-wall models. The results are shown in Table 4. It is observed that for vector and tensor glueballs, the results from the dynamical holographic QCD model are far away from lattice data, especially the masses for higher spin states are too heavy comparing with lattice data. The glueball massea from the hard-wall model are in general lighter than lattice results. Among the three models, the soft-wall model (SW††) with the parameter fixed by the Regge slope can produce reasonable good results comparing with lattice data. However, all models cannot distinguish even and odd parity state for the glueball with the same spin.

In the next section, we will improve the dynamical soft-wall holographic QCD model in order to produce reasonable glueball spectra.

J^{PC}	Lattice	HW1	SW†	SW‡	DSW
0^{-+}	2590	1730	1730	2828	1593
0^{*-+}	3640	3168	2119	3464	2618
0^{--}	5166	3658	2447	4000	10759
1^{+-}	2940	2571	1934	3162	7535
1^{--}	3850	2571	1934	3162	7535
2^{++}	2400	2134	1901	3108	4328
2^{-+}	3100	2134	1901	3108	4328
2^{*-+}	3890	3646	2260	3696	5233
2^{+-}	4140	2927	2201	3598	7830
2^{--}	3930	2927	2201	3598	7830

Table 4. The mass spectra of vector and tensor glueballs in the dynamical soft-wall model, compared with lattice data, and hard-wall model ($z_m = 452$MeV), soft-wall model with SW† indicates μ_G is fixed by lowest mass of 0^{++} glueball, and SW‡ indicates μ_G is fixed by Regge slope of 0^{++} glueball. The unit is in MeV.

5 Glueball spectra in modified dynamical soft-wall holographic QCD model

As we observed from last section that the masses for higher spin glueballs are too heavy comparing with lattice data, while these states are reasonable in the soft-wall model. This indicates that only scalar glueballs are sensitive to the deformed metric, and other glueballs are not excited from this deformed metric background. Therefore we introduce a deformed 5D mass squared for glueballs. In order to distinguish even and odd parity, we introduce the positive and negative coupling between the dilaton field and glueballs, respectively. With this set-up, now the 5D action for the scalar, vector and tensor glueballs $\mathscr{G}(x,z)$ take the following form:

$$S_{\mathscr{G}} = -\frac{1}{2}\int d^5x\sqrt{g_s}e^{-p\Phi}(\ \partial_M\mathscr{G}\partial^M\mathscr{G} + M^2_{\mathscr{G},5}(z)\mathscr{G}^2), \tag{5.1}$$

$$S_V = -\frac{1}{2}\int d^5x\sqrt{g_s}e^{-p\Phi}(\ \frac{1}{2}F^{MN}F_{MN} + M^2_{\mathscr{V},5}(z)\mathscr{V}^2), \tag{5.2}$$

$$\begin{aligned} S_T = -\frac{1}{2}\int d^5x\sqrt{g_s}e^{-p\Phi}(\ & \nabla_L h_{MN}\nabla^L h^{MN} - 2\nabla_L h^{LM}\nabla^N h_{NM} + 2\nabla_M h^{MN}\nabla_N h \\ & -\nabla_M h\nabla^M h + M^2_{h,5}(z)(h^{MN}h_{MN} - h^2)), \end{aligned} \tag{5.3}$$

where $M_5^2(z) = M_5^2 e^{-2\Phi/3}$, $p = 1$ for even parity and $p = -1$ for odd parity.

The equation of motion for any glueball $\mathscr{A}$ can be brought into schrödinger-like equation

$$-\mathscr{A}_n^{''} + V_{\mathscr{A}}\mathscr{A}_n = m^2_{\mathscr{A},n}\mathscr{A}_n, \tag{5.4}$$

with the 5D effective schrödinger potential

$$V_{\mathscr{A}} = \frac{cA_s^{''} - p\Phi^{''}}{2} + \frac{(cA_s^{'} - p\Phi^{'})^2}{4} + e^{2A_s - \frac{2}{3}\Phi}M^2_{\mathscr{A},5}, \tag{5.5}$$

where $c = 1$ for 1-form and $c = 3$ for 0-form and 2-form, and $M^2_{\mathscr{A},5}$ is the value given in Table 1.

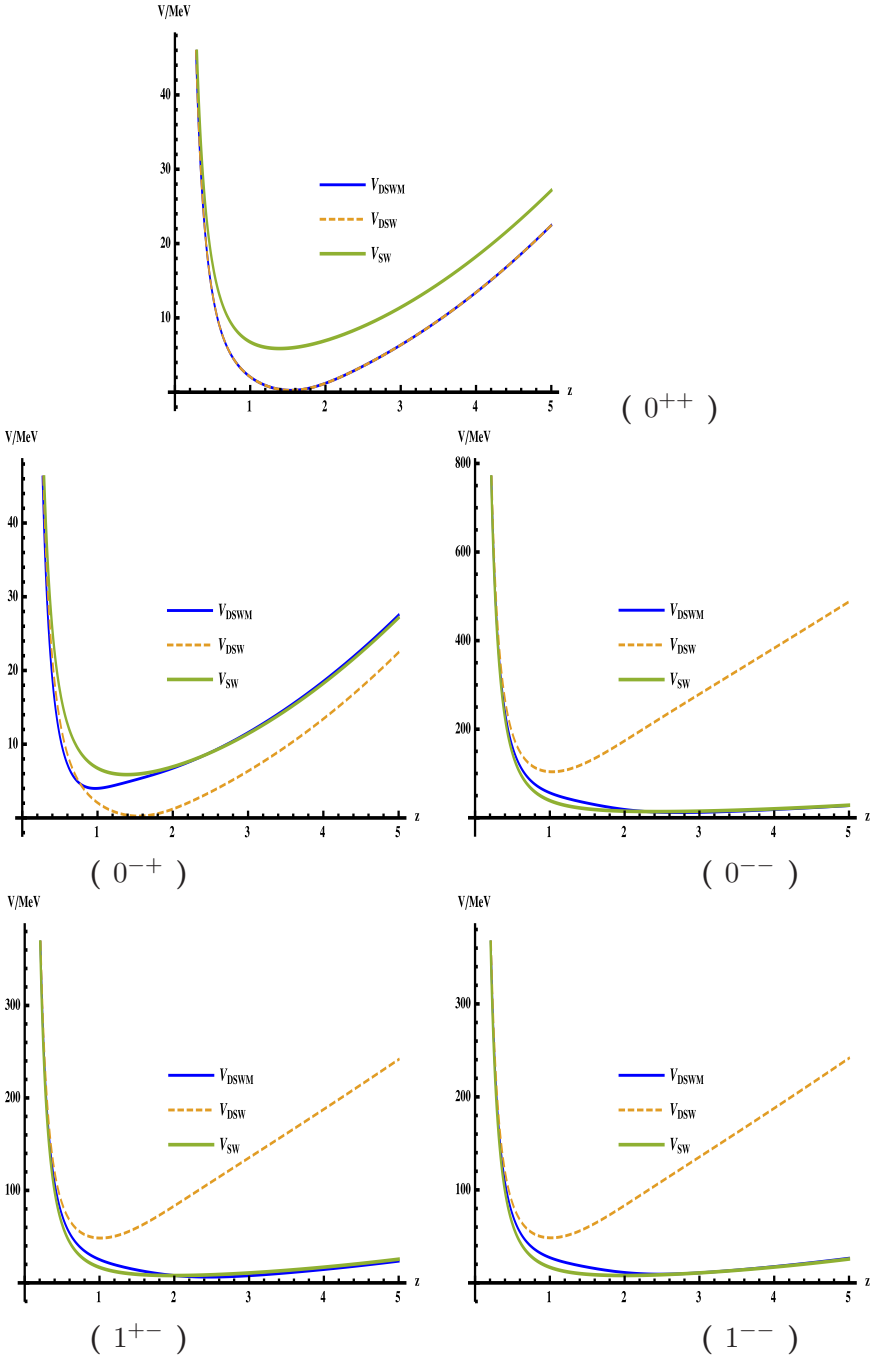

Figure 1. The effective schrödinger potential V of scalar and vector glueballs in the soft-wall model (green thick line), dynamical soft-wall model (orange dashed line) and dynamical soft-wall model with modified M_5^2(blue line).

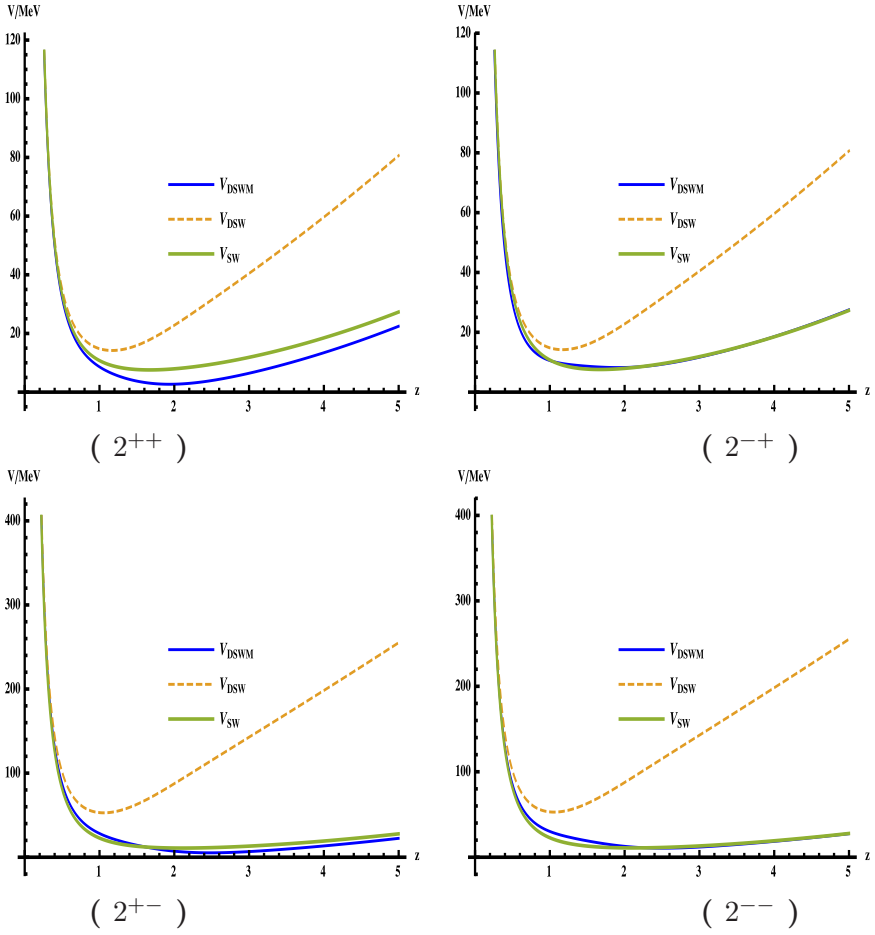

Figure 2. The effective schrödinger potential V of tensor glueballs in the soft-wall model (green thick line), dynamical soft-wall model (orange dashed line) and dynamical soft-wall model with modified M_5^2(blue line).

Compare the 5D effective schrödinger potential Eq.(5.5) with Eqs.(4.4), (4.8) and (4.13), we can see the effect of the deformed 5D mass square $M_5^2(z) = M_5^2 e^{-2\Phi/3}$ is to counteract the deform metric background. In Fig. 1 and Fig. 2, we show the 5D effective schrödinger potential Eq.(5.5) as a function of z and compare with results from the soft-wall model and the original dynamical soft-wall model. It is found that at infrared (IR), except the scalar glueball 0^{++}, the 5D effective schrödinger potential for other glueballs in the modified dynamical soft-wall holographic QCD model coincide with those from soft-wall model. The parity difference $p = \pm$ only brings the difference of the 5D effective schrödinger potential in the range of $0.5 < z < 2$.

The final results of the glueball spectra in the modified dynamical holographic QCD model are shown in Fig. 3 and in Table 5 with details. It is found that with only one parameter $\mu_G = 1$GeV, which is fixed by the Regge slope of the scalar gluball spectra, one can produce other glueballs spectra agree well with lattice data, except three trigluon glueball states 0^{--}, 0^{+-} and 2^{+-}, whose masses are 1.5 GeV lighter than lattice results.

Considering that we only take the simplest quadratic dilaton profile, which corresponds to dimension-2 gluon condensate (or effectively two-gluon condensate) in the vacuum, our results might indicate that these three trigluon glueballs 0^{--}, 0^{+-} and 2^{+-} are dominated by three-gluon condensate contribution.

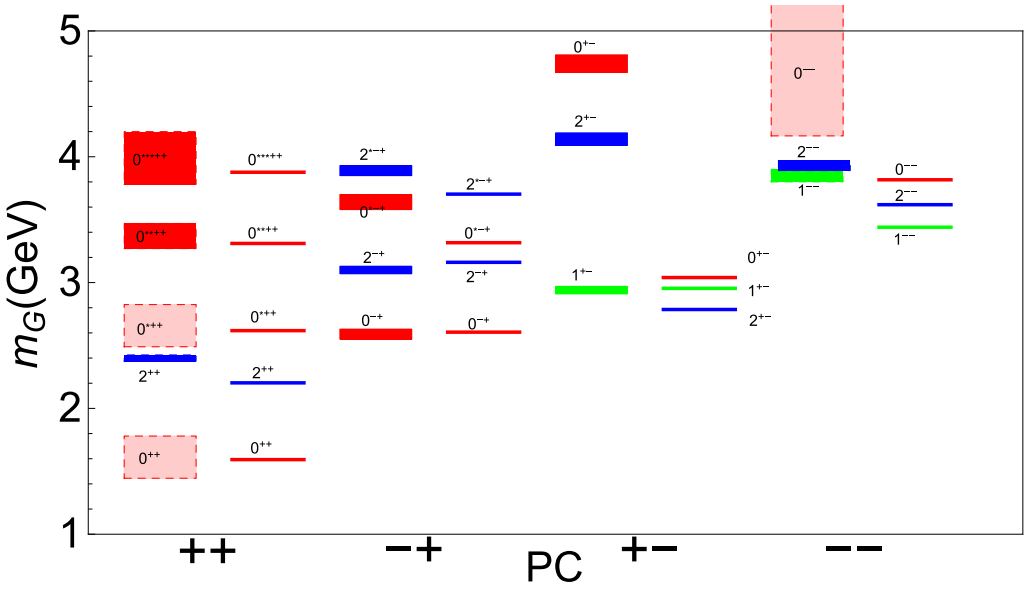

Figure 3. The mass spectra of glueballs in the modified dynamical soft-wall model with $\mu = 1$ GeV (line) compared with the lattice result [2–6] (rectangle).

6 Conclusion and discussion

In this work, we study scalar, vector and tensor glueball spectra in the framework of 5-dimension dynamical holographic QCD model, where the metric structure is deformed self-consistently by the dilaton field. It is found that only scalar glueballs are excited from this deformed metric background, and other glueballs excited from this deformed metric background are much heavy comparing with lattice data. Therefore, for higher spin glueballs, we introduce a deformed 5-dimension mass in order to counteract the effect of the deformed metric background. In order to distinguish glueballs with even and odd parities, we introduce the positive and negative coupling between the dilaton field and glueballs.

With these set-ups, we calculate the glueball spectra with only one free parameter in the dynamical holographic QCD model, which is fixed by the scalar glueball spectra. It is found that all two-gluon glueball spectra produced in the dynamical holographic QCD model are in good agreement with lattice data. We investigate six trigluon glueballs, among these trigluon glueballs, the produced masses for $1^{\pm-}$ and 2^{--} are in good agreement with lattice data, and the produced masses for 0^{--}, 0^{+-} and 2^{+-} are around 1.5 GeV lighter than lattice results. Considering that we only take the simplest quadratic dilaton profile,

J^{PC}	LQCD	Flux tube model	QCDSR	MDSM
0^{++}	1.475-1.73	1.52	1.5	1.593
0^{*++}	2.67-2.83	2.75	–	2.618
0^{**++}	3.37	–	–	3.311
0^{***++}	3.99	–	–	3.877
0^{-+}	2.59	2.79	2.05	2.606
0^{*-+}	3.64	–	–	3.317
0^{--}	5.166	2.79	3.81	3.817
0^{+-}	4.74	2.79	4.57	3.04
0^{++}§	–	–	3.1	2.667
1^{+-}	2.94	2.25	–	2.954
1^{--}	3.85	–	–	3.44
2^{++}	2.4	2.84	2	2.203
2^{-+}	3.1	2.84	–	3.161
2^{*-+}	3.89	–	–	3.703
2^{+-}	4.14	2.84	6.06	2.786
2^{--}	3.93	2.84	–	3.619

Table 5. The mass of glueball spectra in Lattice QCD [2–6], Flux tube model [7], QCDSR [9, 10, 35, 37–39] and modified dynamical soft-wall model. Note that 0^{++}§ is trigluonium. The unit is in GeV.

which corresponds to dimension-2 gluon condensate (or effectively two-gluon condensate) in the vacuum, our results might indicate that the three trigluon glueballs 0^{--}, 0^{+-} and 2^{+-} are dominated by three-gluon condensate contribution. Further studies with more complicated dilaton profile are needed.

Acknowledgement

We thank Danning Li, Hao Ouyang, Cong-Feng Qiao and Liang Tang for useful discussions. This work is supported by the NSFC under Grant Nos. 11175251 and 11275213, DFG and NSFC (CRC 110), CAS key project KJCX2-EW-N01, K.C.Wong Education Foundation, and Youth Innovation Promotion Association of CAS.

References

[1] M. Gell-Mann, Acta Phys. Austriaca Suppl. **9** (1972) 733.

[2] C. J. Morningstar and M. J. Peardon, "The Glueball spectrum from an anisotropic lattice study," Phys. Rev. D **60** (1999) 034509 [hep-lat/9901004].

[3] B. Lucini and M. Teper, "SU(N) gauge theories in four-dimensions: Exploring the approach to N = infinity," JHEP **0106** (2001) 050 [hep-lat/0103027].

[4] H. B. Meyer, "Glueball regge trajectories," hep-lat/0508002.

[5] Y. Chen, A. Alexandru, S. J. Dong, T. Draper, I. Horvath, F. X. Lee, K. F. Liu and N. Mathur *et al.*, "Glueball spectrum and matrix elements on anisotropic lattices," Phys. Rev. D **73** (2006) 014516 [hep-lat/0510074].

[6] E. Gregory, A. Irving, B. Lucini, C. McNeile, A. Rago, C. Richards and E. Rinaldi, JHEP **1210**, 170 (2012) [arXiv:1208.1858 [hep-lat]].

[7] N. Isgur and J. E. Paton, Phys. Rev. D **31**, 2910 (1985).

[8] T. Huang, H. Y. Jin and A. L. Zhang, Phys. Rev. D **59**, 034026 (1999) [hep-ph/9807391].

[9] C. -F. Qiao and L. Tang, "Finding the 0^{--} Glueball," Phys. Rev. Lett. **113**, 221601 (2014).

[10] C. F. Qiao and L. Tang, arXiv:1509.00305 [hep-ph].

[11] V. Mathieu, N. Kochelev and V. Vento, arXiv:0810.4453 [hep-ph]; E. Klempt and A. Zaitsev, Phys. Rept. **454**, 1 (2007); C. Amsler and N. A. Tornqvist, Phys. Rept. **389**, 61 (2004).

[12] J. M. Maldacena, "The Large N limit of superconformal field theories and supergravity," Adv. Theor. Math. Phys. **2**, 231 (1998) [hep-th/9711200].

[13] S. S. Gubser, I. R. Klebanov and A. M. Polyakov, "Gauge theory correlators from noncritical string theory," Phys. Lett. B **428**, 105 (1998) [hep-th/9802109].

[14] E. Witten, "Anti-de Sitter space and holography," Adv. Theor. Math. Phys. **2**, 253 (1998) [hep-th/9802150].

[15] O. Aharony, S.S. Gubser, J. Maldacena, H. Ooguri, Y. Oz, *Large N Field Theories, String Theory and Gravity,* Phys.Rept. 323(2000) 183; O. Aharony, arXiv:hep-th/0212193; A. Zaffaroni, PoS **RTN2005**, 005 (2005); J. Erdmenger, N. Evans, I. Kirsch and E. Threlfall, Eur. Phys. J. A **35**, 81 (2008), [arXiv:0711.4467 [hep-th]].

[16] P. Kovtun, D. T. Son and A. O. Starinets, "Viscosity in strongly interacting quantum field theories from black hole physics," Phys. Rev. Lett. **94**, 111601 (2005) [arXiv:hep-th/0405231].

[17] J. Erlich, E. Katz, D. T. Son and M. A. Stephanov, Phys. Rev. Lett. **95**, 261602 (2005);

[18] A. Karch, E. Katz, D. T. Son and M. A. Stephanov, Phys. Rev. D **74** (2006) 015005.

[19] T. Sakai and S. Sugimoto, Prog. Theor. Phys. **113**, 843 (2005); Prog. Theor. Phys. **114**, 1083 (2006); G. F. de Teramond and S. J. Brodsky, Phys. Rev. Lett. **94**, 201601 (2005);L. Da Rold and A. Pomarol, Nucl. Phys. B **721**, 79 (2005);K. Ghoroku, N. Maru, M. Tachibana and M. Yahiro, Phys. Lett. B **633**, 602 (2006); O. Andreev, V.I. Zakharov, arXiv:hep-ph/0703010; Phys. Rev. D **74**, 025023 (2006); M. Kruczenski, L. A. P. Zayas, J. Sonnenschein and D. Vaman, JHEP **06**, 046 (2005); S. Kuperstein and J. Sonnenschein, JHEP**11**, 026 (2004). H. Forkel, M. Beyer and T. Frederico, JHEP **0707**, 077 (2007);

[20] Deog Ki Hong, Takeo Inami, and Ho-Ung Yee, Phys. Lett. B646:165-171, 2007; Kanabu Nawa, Hideo Suganuma, and Toru Kojo, Phys.Rev.D75:086003, 2007; Deog Ki Hong, Mannque Rho, Ho-Ung Yee, and Piljin Yi, Phys.Rev.D76:061901, 2007.

[21] C. Csaki, H. Ooguri, Y. Oz and J. Terning, JHEP **9901** (1999) 017. R. de Mello Koch, A. Jevicki, M. Mihailescu and J. P. Nunes, Phys. Rev. D **58** (1998) 105009; M. Zyskin, Phys. Lett. B **439** (1998) 373; J. A. Minahan, JHEP **9901** (1999) 020; C. Csaki, Y. Oz, J. Russo and J. Terning, Phys. Rev. D **59** (1999) 065012. R. Apreda, D. E. Crooks, N. J. Evans and M. Petrini, JHEP **0405** (2004) 065.

[22] R. C. Brower, S. D. Mathur and C. I. Tan, Nucl. Phys. B **587** (2000) 249;

[23] H. Boschi-Filho and N. R. F. Braga, JHEP **0305** (2003) 009; H. Boschi-Filho and N. R. F. Braga, Eur. Phys. J. C **32** (2004) 529; H. Boschi-Filho, N. R. F. Braga and H. L. Carrion, Phys. Rev. D **73**, 047901 (2006);

[24] P. Colangelo, F. De Fazio, F. Jugeau and S. Nicotri, "On the light glueball spectrum in a holographic description of QCD," Phys. Lett. B **652**, 73 (2007) [hep-ph/0703316]. L. Bellantuono, P. Colangelo and F. Giannuzzi, "Holographic Oddballs," arXiv:1507.07768 [hep-ph].

[25] H. Forkel, 'Holographic glueball structure," Phys. Rev. D **78**, 025001 (2008) [arXiv:0711.1179 [hep-ph]].

[26] T. Sakai and S. Sugimoto, Prog. Theor. Phys. **113**, 843 (2005); Prog. Theor. Phys. **114**, 1083 (2006).

[27] K. Hashimoto, C. I. Tan and S. Terashima, Phys. Rev. D **77**, 086001 (2008) [arXiv:0709.2208 [hep-th]]. F. Brnner, D. Parganlija and A. Rebhan, Phys. Rev. D **91**, no. 10, 106002 (2015) [arXiv:1501.07906 [hep-ph]]. F. Brnner and A. Rebhan, Phys. Rev. Lett. **115**, no. 13, 131601 (2015) [arXiv:1504.05815 [hep-ph]].

[28] D. Li, M. Huang and Q. -S. Yan, Eur. Phys. J. C **73**, 2615 (2013) [arXiv:1206.2824 [hep-th]].

[29] D. Li and M. Huang, JHEP **1311**, 088 (2013) [arXiv:1303.6929 [hep-ph]].

[30] D. Li and M. Huang, arXiv:1311.0593 [hep-ph].

[31] D. Li, J. Liao and M. Huang, Phys. Rev. D **89**, no. 12, 126006 (2014) [arXiv:1401.2035 [hep-ph]].

[32] D. Li, S. He and M. Huang, JHEP **1506**, 046 (2015) [arXiv:1411.5332 [hep-ph]].

[33] K. Chelabi, Z. Fang, M. Huang, D. Li and Y. L. Wu, arXiv:1511.02721 [hep-ph].

[34] Jaffe R. L., Phys. Rev. D, 1977, **15**: 267

[35] K. F. Liu, Prog. Theor. Phys. Suppl. **168**, 160 (2007); Liu K. F., Wong C. W., Phys. Lett. B, 1981, **107**: 391 Cheng H. Y., Chua C. K., Liu K. F., Phys. Rev. D, 2006, **74**: 094005; 't Hooft G., Isidori G., et al, Phys. Lett. B, 2008, **662**: 424; Zhao Q., Zou B. s., Ma Z. b., Phys. Lett. B, 2005, **631**: 22; Bugg D. V., Peardon M. J., Zou B. S., Phys. Lett. B, 2000, **486**: 49; Narison S., Nucl.Phys.Proc.Suppl., 2009, **186**:306-311.

[36] B. A. Li, Phys. Rev. D **81**, 114002 (2010) [arXiv:0912.2323 [hep-ph]]. H. Y. Cheng, AIP Conf. Proc. **1257**, 477 (2010) [arXiv:0912.3561 [hep-ph]]. S. Janowski, F. Giacosa and D. H. Rischke, Phys. Rev. D **90**, no. 11, 114005 (2014) [arXiv:1408.4921 [hep-ph]]. W. I. Eshraim, arXiv:1509.09117 [hep-ph]. S. He, M. Huang and Q. S. Yan, Phys. Rev. D **81**, 014003 (2010) [arXiv:0903.5032 [hep-ph]]. T. K. Mukherjee, M. Huang and Q. S. Yan, Phys.

Rev. D **86**, 114022 (2012) [arXiv:1203.5717 [hep-ph]]. T. K. Mukherjee and M. Huang, Phys. Rev. D **89**, no. 7, 076002 (2014) [arXiv:1311.1313 [hep-ph]].

[37] S. Narison and G. Veneziano, Int. J. Mod. Phys. A **4**, 2751 (1989). doi:10.1142/S0217751X89001060

[38] J. I. Latorre, S. Narison and S. Paban, Phys. Lett. B **191**, 437 (1987). doi:10.1016/0370-2693(87)90636-8

[39] S. Narison, Nucl. Phys. B **509**, 312 (1998) doi:10.1016/S0550-3213(97)00562-2 [hep-ph/9612457].